

# Composite Nonlinear Feedback Control of a Jib Trolley of a Tower Crane\*

Veli-Pekka Pyrhonen, *Student Member, IEEE* and Matti K. Vilkkö, *Member, IEEE*

**Abstract**—Cranes are required to lift and carry loads swiftly to desired positions without causing excessive swaying motion of the load. These are conflicting requirements, which make feedback control of crane systems challenging. Furthermore, variations in rope length and load mass complicate controller design, since they significantly influence swaying dynamics. This paper considers automatic control of Quanser 3DOF tower crane system using composite nonlinear feedback (CNF) methodology. To be more specific, a CNF controller is designed for the jib trolley position of the crane using partial state measurements. The performance of the CNF controller is compared with Quanser's built-in linear quadratic regulator (LQR) controller both in simulation and experimental setups. The results show that the CNF controller provides better load handling capability in terms of fast positioning of the jib trolley and damping of load swaying.

## I. INTRODUCTION

Cranes are commonly found in industrial sites such as ports, railway yards, pulp and paper mills, manufacturing facilities, construction sites and other work locations. Cranes are used to move hanging loads to desired positions preferably as fast as possible without causing excessive swaying motion of the load. The swaying motion of the load must be managed by carefully coordinated movements of the crane and its components, which require well-developed skills from human operators. Accidents such as damaged surroundings, damaged goods and injuries to people may result, if crane operation fails.

Furthermore, manual crane operation has been reported to cause low efficiency, slow transfer time, and to require long training times of operators, which are cost related matters [1], and, as such, have driven research on automatic crane control. Yet, automatic crane control is a difficult task not only because of the conflicting requirements on fast positioning and small swaying motion of the load, but also due to the variations of load mass and rope length. For example, the height of the load influences to swaying frequency, which may cause feedback loop to generate fast-changing and excessive control actions, which may result in instability. Cranes are also underactuated systems with less control inputs than degrees of freedom. Such features make feedback control of cranes challenging, and hence, a rich variety of control strategies has been adopted for crane automation: In [2–3], input shaping techniques that rely on command filtering techniques has been proposed to reduce payload swaying, whereas gain-scheduling has been applied

in [4] to mitigate the adverse effects of varying rope length. Linear quadratic regulator (LQR) for crane control has been attempted in [5–6],  $H_\infty$  control in [7], and adaptive fuzzy sliding control in [8–9]. Composite nonlinear feedback (CNF) methodology has previously been applied to gantry crane systems in [10–11]; however, those papers assume that full-state is directly available for feedback control, which is impractical. Furthermore, in [10–11], only simulation results are presented, and the controllers have been designed without integration action, which make closed-loop control systems vulnerable for exogenous disturbances. In this paper, jib trolley position of Quanser 3DOF crane system is controlled using CNF methodology with partial state measurements. The controller is also supplemented with a jib trolley velocity reference, which improves closed-loop tracking performance.

CNF is a well-known control design methodology that attempts to achieve simultaneous fast command following and robustness under limited control authority. The CNF was originally proposed by Lin et al. [12] for a class of second order systems. Chen et al. [13] generalized the results of [12] to cover more general systems with measurement feedback. Multivariable case is studied in [14–15], whereas CNF control for a class of nonlinear systems is studied in [16]. Furthermore, Cheng et al. [17] have generalized CNF control for tracking general references, whereas Pyrhonen [18] provided design framework for improving the transient stage of CNF control using general dynamic feedforward set point filters. The CNF methodology produces feedback controllers that consists of parallel-connected linear and nonlinear parts, which can be designed as follows. First, the linear part is designed such that the resulting closed-loop system yields a step response with short rise time and large overshoot. Then, the nonlinear part is designed, which is able to dampen the overshoot tendency caused by the linear part. As a result, the step response of the closed-loop system maintains short rise time, while the overshoot caused by the linear part is reduced. Overshoot is reduced, because CNF controllers are able to use more control effort at the late stage of the transient response, which eventually shortens the settling time of closed-loop systems. This property makes CNF methodology feasible for many control applications requiring fast and precise command following, see for example: [19–23].

The material in this paper is organized as follows. In Section II, a mathematical model of the jib system is developed, which is suitable for control system design. A step-by-step design procedure of CNF control is reviewed in Section III. Then, in Section IV, LQR and CNF controllers are designed for the jib trolley position control of Quanser 3DOF tower crane system with fixed rope length. The results in Section IV indicate that the CNF control provides better load handling capability compared with the LQR control.

\*Research supported by TUT Foundation.

V.-P. Pyrhonen and M. Vilkkö are with the Unit of Automation Technology and Mechanical Engineering, Tampere University, Korkeakoulunkatu 6, 33720, Tampere, Finland. (e-mail: veli-pekka.pyrhonen@tuni.fi, matti.vilkkö@tuni.fi)

## II. JIB SYSTEM MODELING

In this paper, the following class of SISO (Single-Input-Single-Output) systems with input nonlinearity are considered

$$\begin{cases} \dot{x} = Ax + B\text{sat}(u) \\ y = C_y x \\ m = C_m x \end{cases}, \quad x(0) = x_0, \quad (1)$$

where  $x \in \mathbb{R}^n$ ,  $u \in \mathbb{R}$ ,  $y \in \mathbb{R}$  and  $m \in \mathbb{R}^p$ ,  $p \leq n$ , are the state, control input, controlled output, measured output, and where  $x_0$  is an initial condition. The input nonlinearity in (1) is represented by

$$\text{sat}(u) = \min\{u_{\max}, |u|\} \text{sgn}(u), \quad (2)$$

where  $u_{\max}$  is the saturation limit of the input and  $\text{sgn}$  denotes the sign function. Furthermore, the following assumptions on the system matrices of (1) are assumed to be true:

A1: the pair  $(A, B)$  is stabilizable;

A2: the triple  $(A, B, C_y)$  is invertible and has no invariant zeros at the origin;

A3: the pair  $(A, C_m)$  is detectable;

A4: the controlled output  $y$  is a subset of  $m$  i.e.  $y$  is also measured.

Next, a two-dimensional model of the jib system is presented assuming the payload is attached to the trolley using a fixed-length rope. It is further assumed that the tower remains in fixed angular position, which means that the payload sways parallel to the jib when the trolley is moved. The schematic diagram of the crane and its jib system is depicted in Fig. 1.

The trolley is attached to a motorized belt-pulley device, which moves the trolley horizontally along the jib. As indicated in Fig. 1, the trolley moves in positive direction when it travels towards the end of the jib i.e. towards right in Fig. 1. The payload is joined to the trolley with a thin steel cable. Assuming the cable is rigid, the payload can be modeled as a suspended pendulum that swings. When the trolley is moved in positive direction, the payload turns in clockwise direction, and the pendulum angle  $\gamma$  increases positively. Hence, the position of the payload's center of mass in Cartesian coordinate system  $(x, y)$  of Fig. 1 is

$$\begin{cases} x_p(t) = x_j(t) - l_p \sin(\gamma(t)) \\ y_p(t) = -l_p \cos(\gamma(t)) \end{cases}. \quad (3)$$

For simplicity, only the linear state-space model of the jib system is presented, which is suitable for feedback control design. Interested readers may refer to Quanser's manual [6] for complete derivation of the nonlinear equations of motion, which are based on Lagrange method. When the rotational kinetic energy of the pendulum is neglected, the dynamics of the jib system can be written in the form (1) with

$$x^T = [x_j(t), \gamma(t), \dot{x}_j(t), \dot{\gamma}(t)]^T, \quad (4)$$

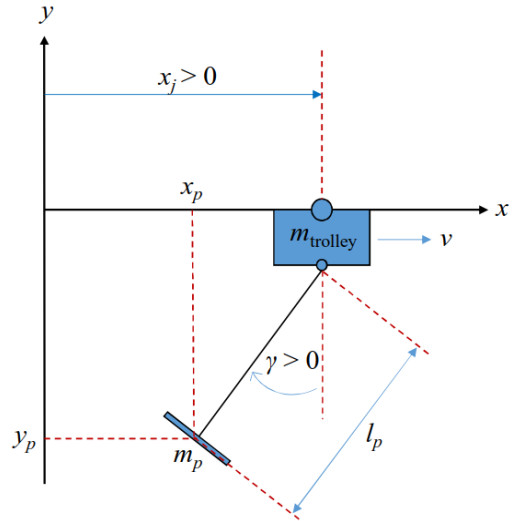


Figure 1. Schematic free-body diagram of the jib system.

$$A = \begin{bmatrix} 0 & 0 & 1 & 0 \\ 0 & 0 & 0 & 1 \\ 0 & a_{32} & 0 & 0 \\ 0 & a_{42} & 0 & 0 \end{bmatrix}, \quad B = \begin{bmatrix} 0 \\ 0 \\ b_3 \\ b_4 \end{bmatrix}, \quad (5)$$

$$C_y = [1 \quad 0 \quad 0 \quad 0], \quad C_m = \begin{bmatrix} 1 & 0 & 0 & 0 \\ 0 & 1 & 0 & 0 \end{bmatrix}, \quad (6)$$

where

$$a_{32} = -\frac{m_p \cdot r_{j,pulley}^2 \cdot g}{m_{trolley} \cdot r_{j,pulley}^2 + J_\psi \cdot K_{g,j}^2}, \quad (7)$$

$$a_{42} = -\frac{(m_{trolley} \cdot r_{j,pulley}^2 + m_p \cdot r_{j,pulley}^2 + J_\psi \cdot K_{g,j}^2) \cdot g}{(m_{trolley} \cdot r_{j,pulley}^2 + J_\psi \cdot K_{g,j}^2) \cdot l_p}, \quad (8)$$

$$b_3 = \frac{r_{j,pulley} \cdot \eta_{g,j} \cdot K_{g,j} \cdot \eta_{m,j} \cdot K_{t,j}}{m_{trolley} \cdot r_{j,pulley}^2 + J_\psi \cdot K_{g,j}^2}, \quad (9)$$

$$b_4 = \frac{r_{j,pulley} \cdot \eta_{g,j} \cdot K_{g,j} \cdot \eta_{m,j} \cdot K_{t,j}}{(m_{trolley} \cdot r_{j,pulley}^2 + J_\psi \cdot K_{g,j}^2) \cdot l_p}. \quad (10)$$

The parameters of the jib model are given in Table 1. The jib model has a pair of imaginary poles at  $s = \pm j3.65$  and two poles at the origin. Note that only the trolley position  $x_j$  and the pendulum angle  $\gamma$  are measured and available for feedback control, so the rest of the states must be estimated in order to enable state feedback control. Furthermore, the output of the current amplifier driving the jib trolley motor is physically limited by (2) with  $u_{\max} = 7A$ .

TABLE I. PARAMETERS OF JIB MODEL.

Symbol	Description	Value	Unit
$m_p$	Mass of the payload	0.147	kg
$K_{t,j}$	Cart motor torque constant	0.0396	Nm/A
$J_\psi$	Jib motor equivalent moment of inertia	$9.14 \cdot 10^{-7}$	kg·m <sup>2</sup>
$l_p$	Vertical distance of payload from jib	0.8636	m

Symbol	Description	Value	Unit
$\eta_{g,j}$	Cart motor gearbox efficiency	0.95	
$K_{g,j}$	Cart motor gearbox gear ratio	3.7:1	
$g$	Gravitational acceleration	9.81	m/s <sup>2</sup>
$\eta_{m,j}$	Jib motor efficiency	0.79	
$r_{j,pulley}$	Radius of pulley wheel mount on jib motor	0.0071	m
$m_{trolley}$	Mass of trolley	0.6	kg

### III. CNF CONTROL DESIGN PROCEDURE

Here, CNF control design with an integral action is presented. Integration action within CNF framework was originally proposed by Peng et al. in [21]. Integration can be included into the design procedure by following a common practice of state augmentation. Here, the state of the system (1) is augmented by the following auxiliary state variable

$$\dot{x}_i = k_i(y - r) = k_i C_y x - k_i r, \quad k_i > 0, \quad (11)$$

where  $k_i$  is a scalar to be selected to yield an appropriate initial integration action. Note that (11) is implementable as A4 is assumed to be true.

The resulting augmented system can then be written by

$$\begin{cases} \dot{\bar{x}} = \bar{A}\bar{x} + \bar{B}u + \bar{B}_r r, & \bar{x}(0) = \bar{x}_0 \\ y = \bar{C}_y \bar{x} \\ \bar{m} = \bar{C}_m \bar{x} \end{cases}, \quad (12)$$

where

$$\bar{x} = \begin{bmatrix} x \\ x_i \end{bmatrix}, \quad \bar{x}_0 = \begin{bmatrix} x_0 \\ 0 \end{bmatrix}, \quad \bar{m} = \begin{bmatrix} m \\ x_i \end{bmatrix}, \quad (13)$$

and where

$$\bar{A} = \begin{bmatrix} A & 0 \\ k_i C_y & 0 \end{bmatrix}, \quad \bar{B} = \begin{bmatrix} B \\ 0 \end{bmatrix}, \quad \bar{B}_r = \begin{bmatrix} 0 \\ -k_i \end{bmatrix}, \quad \bar{C}_y = [C_y \quad 0], \quad \bar{C}_m = \begin{bmatrix} C_m & 0 \\ 0 & 1 \end{bmatrix}. \quad (14)$$

It should be noted that A1 and A2 imply that the pair  $(\bar{A}, \bar{B})$  is stabilizable.

Next, a step-by-step design procedure for calculating the gains of the CNF controller is presented. The procedure is partitioned into two separate parts, which are: A) the design of a linear state feedback part, and B) the design of a nonlinear state feedback part.

#### A. Design of Linear State Feedback Part

First, assume that  $C_m = I$ , i.e. that all states of (1) are measured and available for feedback. Furthermore, assume that A1 and A2 are satisfied. Then design a linear full-state feedback law

$$u_L = -K_L \bar{x} + R_s r, \quad (15)$$

where  $K_L$  is the full-state feedback gain and  $r$  is the target step reference. The gain  $K_L$  must be chosen such that

1) all eigenvalues of the matrix  $(\bar{A} - \bar{B}K_L)$  have strictly negative real parts, and

2) the closed-loop system  $\bar{C}_y(sI - \bar{A} + \bar{B}K_L)^{-1}\bar{B}$  has some desired properties e.g., small damping ratio.

The selected feedback gain  $K_L$  is partitioned by

$$K_L = [K_x \quad K_i], \quad (16)$$

where  $K_x$  corresponds to the full-state feedback gain and  $K_i$  to the gain in the integration channel. The chosen  $K_x$  results in the following scalar-valued feedforward gain

$$R_s = -[C_y(A - BK_x)^{-1}B]^{-1}, \quad (17)$$

which ensures that the DC-gain of the error-free model-based linear closed-loop system from the target reference  $r$  to the controlled output  $y$  is one.

#### B. Design of Nonlinear State Feedback Part

First, compute

$$R_d = \begin{bmatrix} (A - BK_x)^{-1}BR_s \\ 0 \end{bmatrix}, \quad (18)$$

and form the desired state:  $\bar{x}_d = R_d \cdot r$ .

Then construct a parallel-connected CNF control law

$$u = u_L + u_N, \quad (19)$$

where  $u_N$  is the nonlinear feedback component given by

$$u_N = \rho(r, y)K_N[\bar{x} - \bar{x}_d] = \rho(r, y)\bar{B}^T P[\bar{x} - \bar{x}_d], \quad (20)$$

with  $P = P^T > 0$ . The function  $\rho(r, y)$  is any nonpositive function locally Lipschitz in  $y$ , which is used to smoothly increase the damping ratio of the closed-loop system when its output  $y$  approaches the target step reference  $r$ . The matrix  $P$  can be computed by solving the Lyapunov equation

$$(\bar{A} - \bar{B}K_L)^T P + P(\bar{A} - \bar{B}K_L) + W = 0 \quad (21)$$

for a given  $W = W^T > 0$ . The solution  $P$  always exists since all eigenvalues of  $(\bar{A} - \bar{B}K_L)$  are in the left-half complex plane.

The following theorem from [13; 21] provides important stability properties for the closed-loop control system consisting of the system (1) and the CNF control law (19).

*Theorem 1.* Consider the system (1), the linear feedback control law (15), and the composite nonlinear feedback control law (19). For any  $\delta \in (0, 1)$ , let  $c_\delta > 0$  be the largest positive scalar satisfying

$$|K_L \bar{x}| \leq u_{\max}(1 - \delta), \quad \forall \bar{x} \in \{\bar{x} : \bar{x}^T P \bar{x} \leq c_\delta\} \triangleq S. \quad (22)$$

Then, the linear closed-loop control system consisting of (1) and (15) tracks a step input  $r$  without saturating the actuator provided that  $\bar{x}(0)$  and  $r$  and satisfy:

$$\tilde{x}(0) \triangleq (\bar{x}(0) - \bar{x}_d) \in S \text{ and } |Hr| \leq \delta u_{\max}, \quad \forall t, \quad (23)$$

where

$$H \triangleq K_L R_d + R_s. \quad (24)$$

Moreover, for any  $\rho(r, y)$  as discussed above, the composite nonlinear feedback law in (19) is able to track a step input  $r$  provided that (23) is satisfied.

Next, a suitable function  $\rho(r, y)$  needs to be chosen that is used to change the closed-loop system dynamics when  $e \rightarrow 0$ . In this paper, the following nonlinear function [13] is adopted

$$\rho(e) = -\beta \left| \exp(-\alpha|e|) - \exp(-\alpha|y(0) - r|) \right|, \quad |e| = |r - y|, \quad (25)$$

where  $e$  is the control error. The tuning parameters  $\alpha > 0$  and  $\beta > 0$  of (25) are chosen such that the closed-loop control system satisfies the desired transient performance requirements i.e. short settling time and small overshoot. When a step experiment is performed, the function (25) is initially set to zero and it will converge, as  $e \rightarrow 0$ , towards

$$\rho_0 = -\beta \left| 1 - \exp(-\alpha|y(0) - r|) \right|. \quad (26)$$

#### IV. CONTROL SYSTEM DESIGN

In this section, feedback controllers are designed for positioning of the jib trolley as fast as possible while at the same time keeping the swaying motion of the payload desirable. Here, desirable payload swaying means that the deflection angle  $\gamma$  is bounded, say by  $|\gamma| \leq \gamma_{\max}$ , and that the swaying motion is quickly dampened in time. Finally, the payload must be positioned at the desired location in the  $(x, y)$  coordinates. Note that fast positioning of the jib trolley and dampening the swaying motion of the payload are conflicting requirements. That is, it is easy to focus only on the fast and accurate positioning of the trolley without caring the swaying motion of the payload. Similarly, it is easy to keep the deflection angle and swaying motion of the payload small by moving the trolley very slowly. Next, the design of Quanser's built-in LQR controller is presented, which has several features that are adopted for CNF controller as well.

##### A. LQR Control

First, the state of the jib system is augmented to include trolley position integrator, which ensures zero steady-state positioning error in actual experiments, and it improves disturbance rejection of closed-loop system. The resulting control law is given by

$$u = -K_L \bar{x}, \quad \bar{x}^T = \left[ x_j(t), \gamma(t), \dot{x}_j(t), \dot{\gamma}(t), \int x_j(t) dt \right]. \quad (27)$$

The gain  $K_L$  is calculated by minimizing the cost function

$$J = \int_0^{\infty} \left( \bar{x}^T(t) \cdot Q \cdot \bar{x}(t) + u^T(t) \cdot R \cdot u(t) \right) \cdot dt, \quad (28)$$

where  $Q \geq 0$  and  $R > 0$  are weighting matrices given by

$$Q = \text{diag}(5, 5, 1, 5, 1) \quad \text{and} \quad R = 0.1. \quad (29)$$

The resulting state feedback gain is

$$K_L \approx [14.1 \quad 34.7 \quad 11 \quad 1.46 \quad 4.47]. \quad (30)$$

However, the given control law requires information on the rate of changes of  $x_j$  and  $\gamma$ , which can be obtained using a state estimator or proper high-pass filters. Quanser has

designed the following first-order high-pass derivative filters for estimating the rate of changes of  $x_j$  and  $\gamma$

$$G_{hp,x}(s) = \frac{\omega_{f,x} \cdot s}{s + \omega_{f,x}}, \quad G_{hp,\gamma}(s) = \frac{\omega_{f,\gamma} \cdot s}{s + \omega_{f,\gamma}}, \quad (31)$$

whereas the trolley position and pendulum angle measurements are passed through the following first-order low-pass filters to smooth out measurement noise

$$G_{lp,x}(s) = \frac{\omega_{f,x}}{s + \omega_{f,x}}, \quad G_{lp,\gamma}(s) = \frac{\omega_{f,\gamma}}{s + \omega_{f,\gamma}}. \quad (32)$$

The cut-off frequencies of the filters (31) and (32) are  $\omega_{f,x} = 2\pi \cdot 50$  and  $\omega_{f,\gamma} = 2\pi \cdot 2.0$ , respectively.

Finally, the state-error feedback controller for actual implementation is given by

$$u = -K_L \cdot \bar{x}_e,$$

$$\bar{x}_e^T = \left[ (x_{j,f}(t) - x_{j,df}(t)), (\gamma_f(t) - 0), \right.$$

$$\left. (\dot{x}_{j,f}(t) - \dot{x}_{j,df}(t)), (\dot{\gamma}_f(t) - 0), \int (x_{j,f}(t) - x_{j,df}(t)) dt \right], \quad (33)$$

where  $\bar{x}_e$  is the estimated error in which  $x_{j,f}(t)$  is the filtered measured position of the trolley and  $x_{j,df}(t)$  is the filtered trolley position set point,  $\gamma_f$  is the filtered measured pendulum angle,  $dx_{j,f}(t)/dt$  is the filtered derivative of the trolley position,  $dx_{j,df}(t)/dt$  is the filtered trolley velocity set point, and  $d\gamma_f/dt$  is the filtered derivative of the pendulum angle.

The filtered trolley velocity set point is provided by the sigmoid block of the QuaRC (Quanser Real-time Control) software library, and it is calculated in derivative-free manner such that  $dx_{j,df}(t)/dt \rightarrow 0$  in time. Also, the trolley position set point is provided through the sigmoid block, and it produces an s-shaped response similar to the output of a second-order low-pass set point filter. Unfortunately, the calculation procedure of these signals is not documented. Nonetheless, the controller (33) can be viewed as a PID-controller acting on the trolley dynamics and as a PD-controller acting on the pendulum dynamics. The same measurements and filtered reference signals are used in the linear part of the CNF.

##### B. CNF Control Design

The CNF control design begins by augmenting an integration action to the system with the gain  $k_i = 4$ . Next, the feedback gains of the linear part are calculated according to step A of Section III. The poles of the initial closed-loop system are placed at

$$s = [-100, -4, -0.7 + j2, -0.7 - j2, -0.5], \quad (34)$$

which yield the following state feedback gain

$$K_L = [K_x \quad K_i], \approx [11.14 \quad 18.28 \quad 5.90 \quad -0.08 \quad 1.08] \quad (35)$$

and the reference tracking gain given by

$$R_s \approx 11.14. \quad (36)$$

Then the nonlinear part is designed by first calculating  $R_d$  from (18), which yields

$$R_d = [1 \ 0 \ 0 \ 0 \ 0]^T. \quad (37)$$

The gains of the nonlinear part are calculated using (21) by selecting  $W = \text{diag}([1 \ 100 \ 10 \ 5 \ 2])$ , which yield

$$P \approx \begin{bmatrix} 39.72 & -4.53 & 11.20 & -9.53 & 8.42 \\ -4.53 & 48.47 & 3.02 & -2.41 & -1.23 \\ 11.20 & 3.02 & 8.29 & -7.03 & 2.24 \\ -9.53 & -2.41 & -7.03 & 6.02 & -1.89 \\ 8.42 & -1.23 & 2.24 & -1.89 & 3.40 \end{bmatrix}. \quad (38)$$

Thus, the feedback gains of the nonlinear part are

$$K_n \approx [3.07 \ 4.21 \ 2.75 \ -1.06 \ 0.92]. \quad (39)$$

Finally, the tuning parameters of the nonlinear function (25) are chosen as  $\alpha = 5$  and  $\beta = 8$ , which would result in satisfactory tracking performance.

## V. SIMULATION AND EXPERIMENTAL RESULTS

Here, the performances of the designed feedback controllers are tested both in simulation and experimental setups. The control systems should move the trolley from the given initial position to the final position as fast as possible without large pendulum swaying. The pendulum swaying should also be quickly dampened such that the load will finally rest in the vicinity of the target set point.

### A. Simulation Results

Here, the trolley is moved 0.3 meters from its initial position. The positioning performance of the closed-loop systems using LQR and CNF laws are depicted in Fig. 2 and in Fig. 3, respectively, whereas the motor input currents are depicted in Fig. 4. The motor input currents have been obtained by multiplying the controller outputs by 10 because of the current amplifier. The input currents are well below the saturation limits since the trolley motor is quite powerful. The step reference has been activated at  $t = 1$  seconds, and it has been processed by the sigmoid block of QuARC to smoothen trolley movements.

Judging from Fig. 2, the trolley and payload settle to the new resting position in 6 seconds using LQR. In contrast, the CNF controller is able to move the trolley and the load to the new position in 4 seconds, which is notably faster compared with the LQR. Note that both controllers use about the same amount of control effort initially, but the CNF uses more control at the late stage of the transient, which reduces overshoot of the trolley positioning but causes larger momentary pendulum swing. However, the CNF controller brings the trolley quite differently near the target set point when  $e \rightarrow 0$ , and it is able to dampen the payload motion more quickly than the LQR. Note that the response of the strictly linear part of the CNF controller is included in Fig. 3 for easy reference.

### B. Experimental Results

In the actual experiments, software-based watchdogs have been implemented into the Simulink platform, which drives the crane in real time. If too large signals are observed in the system, then watchdogs are triggered, which will stop any experiment. In addition, the fundamental sample time of the platform has been reset from the default value of 0.001s

to 0.002s owing to the slow CPU performance of the testing PC. The tracking performances of the control systems have

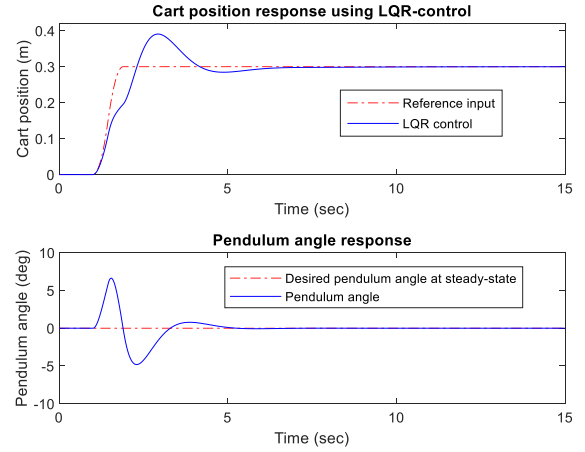


Figure 2. Simulation result: cart position and pendulum angle using LQR.

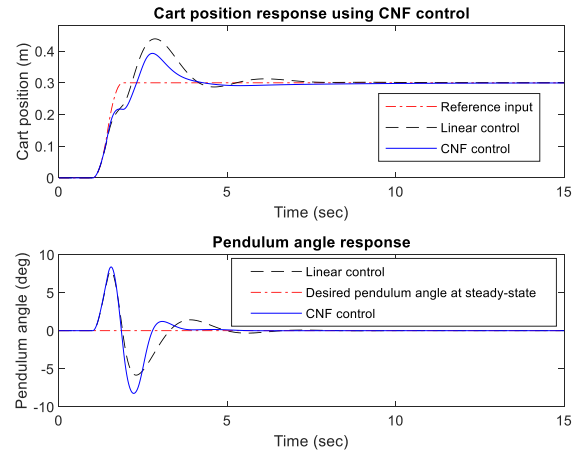


Figure 3. Simulation result: cart position and pendulum angle using CNF.

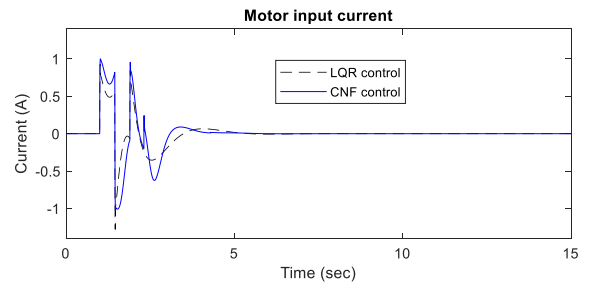


Figure 4. Simulation result: motor input currents.

been depicted in Fig 5. Referring to Fig. 5, both controllers initially move the trolley almost equivalently fast (although CNF is slightly faster) and the initial pendulum sways are identical.

However, the LQR controller settles the trolley too quickly near the target set point, which results in long-term oscillation of the payload. In addition, the integration action of the LQR controller may not be appropriate, since the oscillations are not fully dampened, and the trolley keeps making minor movements back and forth in later time. If the

load is supposed to be automatically placed e.g., in a tight spot, the controller's performance is unacceptable.

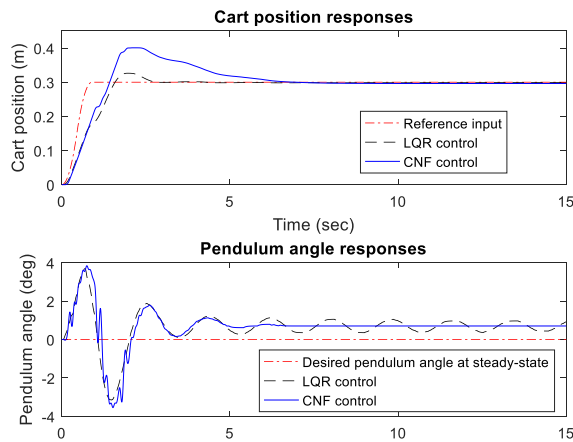


Figure 5. Experimental result: cart position responses and pendulum swaying motions of LQR and CNF.

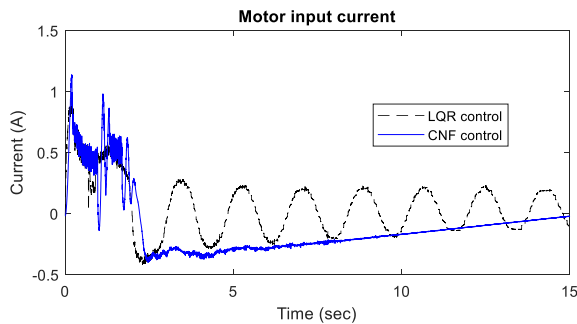


Figure 6. Experimental result: motor input currents.

Conversely, the CNF controller performs well also in the real-time experiments. Interestingly, after the initial part of the step response, the closed-loop control system using CNF controller functions quite differently compared with the system using LQR controller. CNF clearly moves the trolley further and it also brings the trolley more slowly into the vicinity of the target reference. Furthermore, the trolley movements are appropriate as regards to pendulum swaying. Finally, the payload does settle accurately in the given place without oscillation. It should be noted that as the control error becomes small around at  $t = 4$  seconds, the gain of the integration channel of the CNF is enlarged, which enables accurate positioning at the final stage. Such feature cannot be achieved using linear control strategies. It should also be noted that accurate positioning of CNF control and oscillation tendency of LQR control were observed in repeated experiments. Unfortunately, there is a small offset in the pendulum angle measurement, because the angle always converges just below 1 degree in steady state, which is impossible in practice.

## REFERENCES

[1] Y. Fang, B. Ma, P. Wang, and X. Zhang, "A motion planning-based adaptive control method for an underactuated crane system," *IEEE Trans. Contr. Syst. Technol.*, vol. 20, No. 1, pp. 241–248, Jan. 2012.

[2] K. Hekman and W. Singhose, "Feedback control for suppression of crane payload oscillation using on-off commands," in *Proc. Amer. Contr. Conf.*, Jun. 2006, pp. 1784–1789.

[3] S. Garrido, M. Abderrahim, A. Gimnez, R. Diez, and C. Balaguer, "Anti-swinging input shaping control of an automatic construction crane," *IEEE Trans. Autom. Sci. Eng.*, vol. 5, no. 3, pp. 549–557, Jul. 2008.

[4] G. Corrigan, A. Giua, and G. Usai, "An implicit gain-scheduling controller for cranes," *IEEE Trans. Contr. Syst. Technol.*, vol. 6, No. 1, pp. 15–20, Jan. 1998.

[5] J. Jafari, M. Ghazal, M. Nazemizadeh, "A LQR optimal method to control the position of an overhead crane," *Int. J. Robot. and Autom. (IJRA)*, vol. 3, No. 4, Dec. 2014, pp. 1397–1402.

[6] 3DOF Crane, User Manual, Quanser Innovate. Educate., <https://www.quanser.com/products/3-dof-crane/>

[7] I. Burul, F. Kolonic, and J. Matusko, "The control system design of a gantry crane based on  $H_2$  control theory," in *Proc. 33<sup>rd</sup> Int. Convent. MIPRO*, Opatija, Croatia, May 2010, pp. 183–188.

[8] M. Park, D. Chwa, and S. Hong, "Antisway tracking control of overhead cranes with system uncertainty and actuator nonlinearity using an adaptive fuzzy sliding-mode control," *IEEE Trans. Ind. Electron.*, vol. 55, no. 11, pp. 3972–3984, Nov. 2008.

[9] D. Liu, J. Yi, D. Zhao, and W. Wang, "Adaptive sliding mode fuzzy control for a two-dimensional overhead crane," *Mechatronics*, vol. 15, No. 5, pp. 505–522, Jun. 2005.

[10] X. Yu and W. Lan, "Optimal composite nonlinear feedback control for a gantry crane system," in *Proc. 31<sup>st</sup> Annu. IEEE Chin. Contr. Conf.*, Hefei, China, Jul. 2012, pp. 601–606.

[11] X. Yu and W. Lan, "Composite nonlinear feedback control for an underactuated gantry system," in *Proc. 23<sup>rd</sup> Annu. Can. Congr. Appl. Mech.*, Vancouver, BC, Canada, Jun. 2011, pp. 68–71.

[12] Z. Lin, M. Pachter, and S. Banda, "Toward improvement of tracking performance – nonlinear feedback for linear systems," *Int. J. Contr.*, vol. 70, pp. 1–11, Nov. 1998.

[13] B.M. Chen, T.H. Lee, K. Peng, and V. Venkataramanan, "Composite nonlinear feedback control for linear systems with input saturation: theory and an application," *IEEE Trans. Autom. Contr.*, vol. 48, pp. 427–439, Mar. 2003.

[14] M.C. Turner, I. Postletwaite, and D.J. Walker, "Nonlinear tracking control for multivariable constrained input nonlinear systems," *Int. J. Contr.*, vol. 73, no. 12, pp. 1160–1172, Aug. 2000.

[15] Y. He, B.M. Chen, and C. Wu, "Composite nonlinear control with state and measurement feedback for general multivariable systems with input saturation," *Syst. Contr. Lett.*, vol. 54, pp. 455–469, May 2005.

[16] W. Lan, B.M. Chen and Y. He, "On improvement of transient performance in tracking control for a class of nonlinear systems with input saturation," *Syst. Contr. Lett.*, vol. 55, pp. 132–138, Feb. 2006.

[17] G. Cheng, K. Peng, B.M. Chen, and T.H. Lee, "Improving transient performance in tracking general references using composite nonlinear feedback control and its application to high-speed XY-table positioning mechanism," *IEEE Trans. Ind. Electron.*, vol. 54, pp. 1039–1051, Apr. 2007.

[18] V.-P. Pyrhonen and H. J. Koivisto, "On improvement of transient stage of composite nonlinear feedback control using arbitrary order set point filters," in *Proc. 4<sup>th</sup> Annu. IEEE Int. Conf. on Contr. Syst., Comput. and Eng.*, Penang, Malaysia, Nov. 2014, pp. 147–152.

[19] V.-P. Pyrhonen, H.J. Koivisto and M.K. Vilkkö, "A reduced-order two-degree-of-freedom composite nonlinear feedback control for a rotary DC servo motor," in *Proc. 56<sup>th</sup> Annu. IEEE Conf. on Decis. and Contr.*, Melbourne, Australia, Dec. 2017, pp. 2065–2071.

[20] C. Hu, R. Wang, F. Yan, and N. Chen, "Robust composite nonlinear feedback path-following control for underactuated surface vessels with desired-heading amendment," *IEEE Trans. Ind. Electron.*, vol. 63, pp. 6386–6394, May 2016.

[21] K. Peng, B.M. Chen, G. Cheng, and T.H. Lee, "Modeling and compensation of nonlinearities and friction in a microdrive hard disk drive servo system with nonlinear feedback," *IEEE Trans. Contr. Syst. Technol.*, vol. 13, No. 5, pp. 708–721, Sep. 2005.

[22] G. Cheng, and J.-G. Hu, "An observer-based mode switching control scheme for improved position regulation in servomotors," *IEEE Trans. Contr. Syst. Technol.*, vol. 22, pp. 1883–1891, Dec. 2013.

- [23] Z. Hou and I. Fantoni, "Interactive leader-follower consensus of multiple quadrotors based on composite nonlinear feedback control," *IEEE Trans. Contr. Syst. Technol.*, vol. PP, pp. 1–12, Oct. 2017.